Macromolecules
ARTICLE

Macromolecules **2010**, *43*, 10231–10240 **10231**
DOI: 10.1021/ma102101e

A deeper Insight into the Dithiocarbamate Precursor Route: Synthesis of Soluble Poly(thienylene vinylene) Derivatives for Photovoltaic Applications

Hanne Diliën,[†] Arne Palmaerts,[†] Martijn Lenes,[§] Bert de Boer,[§] Paul Blom,[§] Thomas J. Cleij,[†] Laurence Lutsen,[‡] and Dirk Vanderzande*[,†,‡]

[†]*Hasselt University, Institute for Materials Research (IMO), Universitaire Campus, Building D, B-3590 Diepenbeek, Belgium,* [‡]*IMEC, Division IMOMEC, Universitaire Campus, Wetenschapspark 1, B-3590 Diepenbeek, Belgium, and* [§]*Molecular Electronics, University of Groningen, Nijenborgh 4, NL-9747 AG Groningen, The Netherlands*

Received September 10, 2010; Revised Manuscript Received November 4, 2010

ABSTRACT: The synthesis of, two new poly(thienylene vinylene) derivatives is described, i.e. poly(3-octyl-2,5-thienylene vinylene) (O-PTV) and poly(bis[octylphenyl-2,5-thienylene vinylene]) (BOP-PTV). Both polymers have been prepared via the dithiocarbamate (DTC) precursor route. The polymerization protocol of the monomer toward the precursor polymer has been optimized by the use of different bases, leading to improved reproducibility of the polymerization step. Processability has been guaranteed by the introduction of alkyl side chains. Finally the precursor polymers were converted toward conjugated polymers and they were fully characterized by UV/vis, IR, GPC, and cyclic voltammetry. Bulk heterojunction solar cells with PCBM as acceptor showed promising power conversion efficiencies of 0.80% for BOP-PTV and 0.92% for O-PTV.

Introduction

There is a growing need for inexpensive renewable energy sources, polymer solar cells can come up to this demand. During the last decades the development of such photovoltaic cells has progressed rapidly.[1] An important limitation of the currently applied materials is the mismatch between the absorption spectrum of the polymers and the solar emission spectrum AM1.5. The use of low band gap polymers (E_g < 1.8 eV) is a viable method to expand the absorption window of solar cells and therefore increase their efficiency.[2−5] From models it can be estimated that for a classical bulk heterojunction solar cell with a conjugated polymer as a donor in combination with PCBM as an acceptor, a band gap of 1.4 eV for the donor material would be optimal.[6,7] Since π-conjugated polymers allow endless manipulation of their chemical structure, tuning of the band gap of these materials is a research topic of ongoing interest. It is anticipated that this band gap engineering can give the polymer its desired electrical and optical properties. Earlier, it has already been proven that PTV's are interesting conjugated polymers because of their high mobility for charge carriers and low band gap of about 1.7 eV.[8−10]

The synthesis of PTV derivatives can be achieved by many pathways, all with their specific advantages and disadvantages. A first well studied method is the synthesis by condensation reactions, such as Horner−Wadsworth−Emmons coupling.[11] Using this route, only low molecular weights are obtained, which have a negative influence on the morphology of thin films made from these materials. A general method to synthesize poly(arylene vinylene)s and more specifically PTV derivatives, is based on precursor routes. In a precursor route, soluble precursor polymers are first synthesized, which in a next step are converted into their corresponding conjugated polymers. They contain typically a functional group in the main chain that is a precursor for a double bond.[12] Actually the Durham route represents the very first example of such precursor route.[13] Recently a quite new type of precursor route was introduced in which rather the solubilizing side chains on the conjugated backbone are thermally cleaved. This converts the conjugated polymer into an insoluble material and may lead to a substantial stabilization of the nanomorphology of the active layer in bulk heterojunction solar cells.[14,15] A similar advantage can be achieved in principle for the many precursor routes that have been developed over the last decades toward for example PTV derivatives. These routes differ by their functional groups, their polymerization conditions and, more important, their specific benefits. However it is quite a challenge to tune conversion conditions such that in this way a controlled nanomorphology is produced. Consequently, in general and also in this work, preference is given to derivatives that yield a conjugated polymer which maintain solubilizing side chains to guarantee easy processing also after conversion.

The first precursor route toward PTV was based on the Wessling route and has been patented by Harper and West,[16] also Elsenbaumer et al. explored this route.[17,18] Unfortunately unstable precursor polymers, which spontaneous eliminate toward insoluble PTV, were obtained. Later on, the Wessling route has been modified by both Saito[19−21] and co-workers and Murase.[22] Their merit consists of an adaptation of the leaving group in the precursor polymer. The sulfonium group has been replaced by a methoxy leaving group. Because of this modification a precursor polymer which is soluble in organic solvents has been created. A second studied pathway is the sulphinyl precursor route.[23] This pathway has been investigated in our research group, but the monomer synthesis seemed to be very problematic as a result of the instability of the intermediary products toward the monomer. In the search toward stable monomers also the xanthate route has been studied, as well in our research group[24] as by Burn et al.[25]

*To whom correspondence should be addressed at the Hasselt University. Telephone +32 (0) 11 26 83 21. Fax: + 32 (0)11 26 83 01. E-mail: dirk.vanderzande@uhasselt.be.

Published on Web 11/19/2010

Notwithstanding the fact that stable monomers can be formed and moreover that these monomers can be polymerized and converted toward PTV-derivatives, this route had still some drawbacks. First, the polymerizations have a rather low yield and second the obtained polydispersities are high (PD > 15). At last the, in this study discussed, dithiocarbamate route can be used.[26] This procedure has been chosen as the precursor route of preference to make PTVs, since it is the only route which enables to prepare stable monomers from the electron rich thiophene structure. The polymerization of the monomers starts with a base induced elimination leading to the formation of a *p*-quinodimethane system which is the actual monomer. For this elimination, a relative strong and sterically hindered base has to be used. In the past lithium diisopropylamide (LDA) and lithium bis(trimethylsilyl)amide (LHMDS) have been used for this purpose.[27] The use of LDA suffers from a lot of side reactions (cleavage of the alkyl side chain, transfer of the isopropyl group) and the polymerization of 3-alkyl substituted PTVs afford low molecular weight polymers (M_w < 14.000) in low yields (5%).[28] To avoid these side reactions, LHMDS has been used as a base, to achieve greater selectivity. Previous results showed that polymerization using LHMDS, leads to high molecular weights but with a limited reproducibility.[29]

To gain more insight in the polymerizations of these monomers a number of different bases have now been evaluated. Besides LHMDS also the sodium and potassium equivalent of LHMDS (NaHMDS and KHMDS), have been analyzed. The, less sterically hindered, Na*t*BuO has been used as well. The change of base leads to more reproducible results while the precursor polymer still reaches high molecular weights.

After optimization, two new conjugated polymers have been synthesized; poly(3-octyl-2,5-thienylene vinylene) (O-PTV) and poly[3,4-bis(octylphenyl)-2,5-thienylene vinylene] (BOP-PTV). Octyl side chains have been chosen because in the past, it was observed that butyl and hexyl side chains were insufficient to guarantee solubility. The polymers were characterized by means of UV−vis, IR, and cyclic voltammetry, and they were tested on their photovoltaic properties in bulk heterojunction solar cells with PCBM as acceptor.

Experimental Section

General. All the commercially available chemicals were purchased from Acros or Aldrich and were used without further purification unless stated otherwise.

Tetrahydrofuran (THF) and diethyl ether used in the synthesis were dried by distillation from sodium/benzophenone.

Techniques. ^{1}H NMR spectra were taken on a Varian Inova 300 spectrometer. For all synthesized substances spectra were recorded in deuterated chloroform; the chemical shift at 7.24 ppm (relatively to TMS) was used as reference. Molecular weights and molecular weight distributions were determined relative to polystyrene standards (Polymer Laboratories) by size exclusion chromatography (SEC). Chromatograms were recorded on a Spectra series P100 (Spectra Physics) equipped with two MIXED-B columns (10 μm, 30 cm, Polymer Laboratories) and a relative index (RI) detector (Shodex). A THF solution of oxalic acid (1.1×10^{-3} M) was used as the eluent at a flow rate of 1.0 mL/min. Toluene was used as flow rate marker. GC/MS analyses were carried out on TSQ-70 and Voyager mass spectrometers (Thermoquest); capillary column, Chrompack Cpsil5CB or Cpsil8CB. Melting points (uncorrected) were measured with a digital melting point apparatus, Electrothermal IA 9000 series. Fourier transform-infrared spectroscopy (FT-IR) was performed on a Perkin-Elmer Spectrum One FT-IR spectrometer (nominal resolution 4 cm^{-1}, summation of 16 scans). Ultraviolet visible spectroscopy (UV−vis) was performed on a VARIAN CARY 500 UV−vis−NIR spectrophotometer. Thin film electrochemical measurements were performed with an Eco Chemie Autolab PGSTAT 20 potentiostat/galvanostat using a conventional three-electrode cell under N_2 atmosphere (electrolyte: 0.1 M (TBA)PF_6 in anhydrous CH_3CN). For the measurements, an $Ag/AgNO_3$ reference electrode (0.01 M $AgNO_3$ and 0.1 M (TBA)PF_6 in CH_3CN), a platinum counter electrode and an indium−tin oxide (ITO) coated glass substrate working electrode were used. For the measurements, the polymers were deposited by spin coating directly onto the ITO substrates. Cyclic voltammograms were recorded at 50 mV/s. All potentials were referenced using a known standard, ferrocene/ferrocenium, which in CH_3CN solution is estimated to have an oxidation potential of −4.98 eV vs vacuum.

Synthesis of O-PTV. *Monomer Synthesis. 3-Octyl-2,5-dibromothiophene* (***1c***). To a solution of 3-octylthiophene (**1b**) (65 g, 333 mmol) in DMF (200 mL) a solution of *N*-bromosuccinimide (130 g, 733 mmol) in DMF (200 mL) was added slowly at 0 °C via a dropping funnel. The mixture was stirred for 72 h in darkness. The reaction mixture was poured onto a solution of NaOH (300 mL, 2.5 M) and stirred at 0 °C. The mixture was extracted with diethyl ether and the combined organic layers were washed with NaOH (2.5 M) and brine. The organic layers were dried over $MgSO_4$, the solvent was evaporated and product **1c** was obtained as yellow oil (yield 86%, 101 g).

^{1}H NMR ($CDCl_3$): 6.77 (s, 1H), 2.50 (t, J = 7.78, 2H), 1.56−1.46 (m, 2H), 1.28−1.23 (m, 10H), 0.86 (t, J = 1.23, 3H). ^{13}C NMR ($CDCl_3$): 143.0, 130.9, 110.3, 107.9, 31.8, 29.6, 29.5, 29.3, 29.2, 29.1, 22.7, 14.1. MS (EI, *m*/*e*): 352, 354, 356 (M^+).

3-Octyl-2,5-thiophenedicarboxaldehyde (***1d***). In a three-necked round-bottom flask a solution of 2,5-dibromo-3-octylthiophene (**1c**) (35 g, 99 mmol) in THF (100 mL) was stirred under nitrogen atmosphere at −78 °C. A solution of *n*-butyl lithium (135 mL, 215 mmol of a 1.6 M solution in hexane) was slowly added with a cannula, the mixture was stirred for 30 min and afterward 1-formylpiperidine (24.6 g, 217 mmol), freshly distilled, was slowly added. The resulting mixture was stirred for 12 h at room temperature. HCl (2M) was added to quench the excess of *n*-BuLi followed by extraction with chloroform. The organic layers were dried over $MgSO_4$, filtered and the solvent was evaporated. The obtained compound was purified by column chromatography on silica gel with $CHCl_3$/hexane (1/1) as a solvent. The dialdehyde **1d** was obtained as an orange oil (yield 71%, 18 g).

^{1}H NMR ($CDCl_3$): 10.12 (s, 1H), 9.95 (s, 1H), 7.62 (s, 1H), 2.97 (t, J = 7.88, 2H), 1.73−1.63 (m, 2H), 1.31−1.23 (m, 10H), 0.86 (t, J = 7.08, 3H). ^{13}C NMR ($CDCl_3$): 183.4, 183.0, 152.0, 147.8, 143.3, 137.1, 31.8, 31.2, 31.2, 29.2, 29.2, 28.5, 22.6, 14.1. MS (EI, *m*/*e*): 252 (M^+).

2,5-Bis(hydroxymethyl)-3-octylthiophene (***1e***). In a three-necked round-bottom flask a mixture of $LiAlH_4$ (3.8 g, 15 mmol) in dry THF (50 mL) was made under argon atmosphere. This slurry was cooled to 0 °C and a solution of aldehyde **1d** (1.1 g, 0.03 mol) in THF (50 mL) was slowly added with a dropping funnel. When the addition was complete the slurry was heated at reflux temperature for 5 h. Sequently, the mixture was placed in an ice bath and quenched very careful with water and an aqueous 15% NaOH solution. The solution was extracted with diethyl ether, dried over $MgSO_4$ and the solvent was evaporated under reduced pressure. The diol was obtained as a yellow oil in a yield of 73% (5.6 g).

^{1}H NMR ($CDCl_3$): 6.76 (s, 1H), 4.73 (s, 2H), 4.70 (s, 2H), 2.52 (t, J = 8.08, 2H), 1.57−1.47 (m, 2H), 1.28−1.22 (m, 10H), 0.85 (t, J = 6.88, 3H). ^{13}C NMR ($CDCl_3$): 142.3, 140.3, 136.8, 127.7, 60.2, 57.8, 31.9, 31.0, 30.9, 29.4, 29.3, 28.3, 22.6, 14.1. MS (EI, *m*/*e*): 256 (M^+).

2,5-Bis(chloromethyl)-3-octylthiophene (***1f***). To a cooled (0 °C), stirred solution of diol **1e** (4.67 g, 18.2 mmol) in THF (30 mL) was added a solution of $SOCl_2$ (5.41 g, 45.5 mmol) in THF (40 mL). The temperature of the reaction mixture was allowed to increase to room temperature under continuous stirring for 1 h. Then, the mixture was cooled down again at 0 °C and a saturated sodium bicarbonate solution was added dropwise until neutral. The mixture

was extracted with diethyl ether, dried over $MgSO_4$ and filtered. The solvent was evaporated and the highly reactive dichloride **1f** was obtained as an orange oil. Because of the reactivity of **1f**, the dichloride (4.43 g) was used in the next reaction step without purification.

^{1}H NMR ($CDCl_3$): 6,81 (s, 1H) 4.69 (s, 2H), 4.68 (s, 2H), 2.52 (t, J = 7.78, 2H), 1.61−1.51 (m, 2H), 1.32−1.22 (m, 10H), 0.86 (t, J = 7.14, 3H).

Synthesis of 3-Octythiophene-2,5-diylbismethylene N,N-Diethyldithiocarbamate (***1g***). To a solution of bischloromethyl **1f** (4.43 g, 15 mmol) in ethanol (50 mL), sodium diethyldithiocarbamic acid salt trihydrate (13.61 g, 6 mmol) was added as a solid. The mixture was stirred at ambient temperature overnight. Then, water was added and the desired monomer was extracted with diethyl ether and dried over $MgSO_4$. The monomer was obtained after column chromatography (eluent: $CHCl_3$/hexane 1/1) as a yellow oil (75%, 5.8 g).

^{1}H NMR ($CDCl_3$): 6.75 (s, 1H), 4.65 (s, 2H), 4.58 (s, 2H), 4.01 (q, J = 7.06, 4H), 3.69 (q, J = 7.25, 4H), 2.48 (t, J = 7.70, 2H), 1.59−1.47 (m, 2H), 1.29−1.23 (m, 10H), 0.85 (t, J = 7.10, 3H). ^{13}C NMR ($CDCl_3$): 194.7, 194.5, 141.4, 136.9, 130.5, 129.0, 49.5, 49.3, 46.7, 36.9, 35.2, 31.9, 30.7, 29.5, 29.2, 28.4, 22.7, 14.1, 12.5, 11.6.

Precursor Polymer Synthesis

Polymerization. The monomer **1g** (2.8 g, 5.4 mmol) was freeze-dried. A solution, with a monomer concentration of 0.4 M, in dry THF (13.5 mL) was degassed by passing through a continuous nitrogen flow. The solution was cooled to 0 °C. Sodium bis(trimethylsilyl)amide (NaHMDS) (11 mL of a 1 M solution in THF) was added in one go to the stirred monomer solution. The resulting mixture was stirred for 90 min under continuous nitrogen flow at 0 °C. The polymer was precipitated in ice water and the water layer was neutralized with diluted HCl before extraction with chloroform. The solvents of the combined organic layers were evaporated under reduced pressure and a second precipitation was performed in cold methanol. The polymer **1h** was collected and dried *in vacuo* (yield 56%, 1.1 g).

UV−vis: λ_{max} = 261 nm (in film). FT-IR(NaCl disk): 2931, 2846, 1486, 1415, 1268, 1206 cm^{-1}. SEC: $M_w = 86 \times 10^3$. PD = 3.1. ^{1}H NMR ($CDCl_3$): 6.57 (br, 1H), 5.46 (br, 1H), 3.96 (br, 2H), 3.66 (br, 4H), 2.27 (br, 2H), 1.21 (br, 18H), 0.85 (br, 3H). ^{13}C NMR ($CDCl_3$): 193.96, 139.5, 138.8, 133.8, 127.6, 52.7, 48.9, 46.6, 31.8, 30.7, 29.5, 29.3, 28.2, 22.6, 14.0, 12.5, 11.5.

Conjugated Polymer

Thermal Conversion toward O-PTV. The precursor polymer **1h** (1 g, 2.7 mmol) was dissolved in *o*-dichlorobenzene (50 mL) and refluxed for 4.5 h. Afterward the solution was cooled to room temperature and the obtained slurry was precipitated in methanol. The precipitate was filtered off, washed several times with methanol and dried *in vacuo*. A purple/black solid has been obtained (yield 90%, 0.54 g).

UV−vis: λ_{max} = 620 nm (in film). λ_{max} = 582 nm (in $CHCl_3$). FT-IR: 2931, 2846, 1460, 1250, 1016, 926 cm^{-1}. SEC: $M_w = 65 \times 10^3$; PD = 2.6. ^{1}H NMR ($CDCl_3$): 6.97 (s, 1H), 5.00 (s, 1H), 2.26 (br, 2H), 1.24 (br, 12H), 0.85 (br, 3H).

Synthesis of BOP-PTV. *Monomer Synthesis. Synthesis of 3,4-Bis(4-octylphenyl)thiophene* (***2d***). A solution of *p*-octylphenyl boronic acid (**2b**) (4.45 g, 19 mmol), dibromothiophene (**2c**) (1 g, 4.1 mmol), and potassium fluoride (0.96 g, 17 mmol) was made in a mixture of water and toluene (1/1). $Pd(PPh_3)_4$ (0.33 g, 0.029 mmol) was added as a catalyst. The resulting mixture was refluxed for 18 h. Then an extraction was performed with dichloromethane, the organic layers were dried over $MgSO_4$ and the solvent was evaporated in vacuo. The desired product **2d** was obtained as colorless oil after purification by column chromatography over silica with pentane as an eluent (84%, 7.4 g).

^{1}H NMR ($CDCl_3$): 7.27 (s, 2H), 7.11−7.02 (m, 8H), 2.58 (t, J = 7.87, 4H), 1.64−1.54 (m, 4H), 1.34−1.20 (m, 20H), 0.89 (t, J = 6.93, 3H). ^{13}C NMR ($CDCl_3$): 141.7, 141.5, 133.9, 128.8, 128.1, 123.5, 35.6, 31.9, 31.3, 29.5, 29.35, 29.3, 22.7, 14.1. MS (EI, m/e): 460 (M^+).

3,4-Bis(4-octylphenyl)-2,5-bis(chloromethyl)thiophene (***2e***). In a three-necked round-bottom flask, a mixture of **2d** (3.3 g, 7.1 mmol) and paraformaldehyde (0.58 g, 19 mmol) was made. The mixture was cooled to 0 °C under a nitrogen atmosphere, concentrated HCl (4.0 g, 41 mmol) and acetic anhydride (7.3 g, 71 mmol) were added dropwise. The resulting mixture was heated at 75 °C for 4.5 h. After cooling down (0 °C) a cold saturated solution of sodium acetate and a solution of sodium hydroxide (2M) were added. The solution was extracted with diethyl ether, dried over $MgSO_4$ and the solvents were evaporated under vacuo. Because of the instability of the product, the crude product **2e** was used in the next reaction step without further purification.

^{1}H NMR ($CDCl_3$): 7.04−6.92 (m, 8H), 4.68 (s, 4H), 2.57 (t, J = 7.94, 4H), 1.63−1.49 (m, 4H), 1.31−1.22 (m, 20H), 0.86 (t, J = 7.08, 3H).

Synthesis of 3,4-bis(4-octylphenyl)thiophene-2,5-diylbismethylene-N,N-diethyl dithiocarbamate (***2f***). Compound **2e** (3.96 g, 7.1 mmol) was dissolved in methanol (50 mL), sodium diethyldithiocarbamate trihydrate (4.8 g, 21 mmol) was added as a solid and the mixture was stirred overnight. Subsequently the mixture was extracted with diethyl ether, dried over $MgSO_4$ and the solvent was evaporated under vacuo. The crude product was purified by column chromatography with a mixture of chloroform/pentane (1/1) as an eluent. The dithiocarbamate monomer **2f** was obtained as orange oil (yield: 54%).

^{1}H NMR ($CDCl_3$): 7.01−6.87 (m, 8H), 4.62 (s, 4H), 4.06−3.95 (m, 4H), 3.77−3.66 (m, 4H), 2.50 (t, J = 7.58, 4H), 1.60−1.51 (m, 4H), 1.32−1.20 (m, 32H), 0.86 (t, J = 7.16, 3H). ^{13}C NMR ($CDCl_3$): 194.6, 141.5, 141.4, 133.0, 132.7, 130.0, 128.0, 49.4, 46.8, 36.2, 35.6, 31.9, 31.2, 29.5, 22.7, 14.1, 12.5.

Precursor Polymer Synthesis

Polymerization. The monomer **2f** (0.37 g, 0.48 mmol) was freeze-dried. A solution, with a monomer concentration of 0.2 M, in dry THF (2.4 mL) was degassed by passing through a continuous nitrogen flow. The solution was cooled to 0 °C. Sodium bis(trimethylsilyl)amide (NaHMDS) (0.6 mL of a 1 M solution in THF) was added in one go to the stirred monomer solution. The resulting mixture was stirred for 90 min under continuous nitrogen flow at 0 °C. The polymer was precipitated in ice water and the water layer was neutralized with diluted HCl before extraction with chloroform. The solvent of the combined organic layers was evaporated under reduced pressure and a second precipitation was performed in pure cold methanol. The polymer **2g** was collected and dried *in vacuo* (yield: 54%, 0.16 g).

UV−vis: λ_{max} = 242 nm (in film). IR: 2921; 2862; 1485; 1415; 1266; 1207. SEC: $M_w = 186 \times 10^3$. PD = 2.7. ^{1}H NMR ($CDCl_3$): 7.00−6.68 (br, 8H), 4.07−3.93 (br, 4H), 3.91−3.38 (br, 4H), 2.44 (br, 4H), 1.61−1.40 (br, 24H), 1.32−1.15 (br, 12H), 0.91−0.79 (br, 6H).

Conjugated Polymer

Thermal Conversion toward BOP-PTV. The precursor polymer **2g** (0.16 g, 0.25 mmol) was dissolved in *o*-dichlorobenzene (6.2 mL) and stirred for 4,5 h at 150 °C. After being cooled to room temperature, the resulting dark solution was precipitated dropwise in methanol. The conjugated **2f** polymer was filtered off and dried under reduced pressure. A dark blue solid was obtained in a yield of 60% (87 mg).

UV−vis: λ_{max} = 596 nm (in $CHCl_3$ solution); λ_{max} = 601 nm, shoulder at 646 nm (in film). FT-IR: 2930; 2850; 1269; 1095; 1030; 934; 802. SEC: $M_w = 53 \times 10^3$. PD = 2.1. ^{1}H NMR ($CDCl_3$): 6.99−6.80 (br, 8H), 2.54 (br, 4H), 1.61−1.48 (br, 4H), 1.31−1.18 (br, 20 H), 0.89−0.82 (br, 6H).

Device Preparation. All devices were made on prepatterned ITO/Glass samples supplied by Philips. After a standardized cleaning procedure in a wet station, a layer of PEDOT:PSS (poly(3,4-ethylenedioxythiophene) doped with poly(styrenesulfonate) was spin coated on top of the ITO. This layer has a

thickness of 50 to 60 nm. The aqueous PEDOT:PSS solution (CLEVIOS P VP AI 4083 by H. C. Starck) was spin coated in exactly the same way for each substrate (10 s at 500 rpm followed by 50 s at 1500 rpm).

On top of the PEDOT:PSS, a layer of either BOP-PTV or O-PTV was spin coated inside the glovebox. Table 1 shows the spin procedures and concentrations for both polymers. Finally, as a cathode, a metal top contact was evaporated, consisting of 5 nm samarium with 100 nm aluminum on top.

Device Measurements. All measurements were performed in a glovebox, under nitrogen atmosphere. Current versus voltage characteristics were determined using a Keithly 2400 Source meter. The device current was registered using a Labview program, while sweeping a voltage across the device, going up from 0 V to a positive voltage, then down to −2 V and up again to 0 V. The thicknesses of all spin coated polymers, including the PEDOT:PSS were determined using a Dektak 6 M Stylus Profiler.

Results and Discussion

Monomer Synthesis. In view of the advantages compared to other routes (e.g., Wessling, xanthate, ...), the dithiocarbamate (DTC) route has been chosen as the precursor route of preference to obtain the PTV derivatives. The monomers used were synthesized by two different synthetic pathways in accordance with their substitution profile (mono- or disubstituted backbone).[6,30] The mono substituted PTV (O-PTV) has been synthesized by a six-step synthetic procedure (Scheme 1). The synthetic scheme starts with substitution of commercially available 3-bromothiophene (**1a**) by a Kumada coupling.[31] Second, bromination has been performed.[32] Dialdehyde **1d** was formed by a reaction with *n*-BuLi and *n*-formylpiperidine.[33] Reduction with lithium aluminum hydride, followed by chlorination of the diol with thionyl choride afforded intermediate **1f**.[34] Because of the instability of thiophene **1f**, it has to be converted in situ to the dithiocarbamate monomer **1g**.[6] Monomer purification was performed by column chromatography (silica).

Table 1. Applied Spin Coating Procedures and Concentrations for Both Polymers

polymer	solvent	concn (mg/mL)	spin program (lid, speed (rpm), acceleration (rpm/s), time (s))
BOP-PTV	$CHCl_3$	15	close, 300, 500, 4 close, 500, 500, 60 open, 500, 500, 30
O-PTV	*o*-dichlorobenzene	10	open, 300, 100, 120 open, 800, 200, 30

For the BOP-PTV monomer a slightly different pathway has been used (Scheme 2). The monomer has been formed in a 4 step synthesis. The first step is the synthesis of boronic acid[35] **2b** which is used for the formation of 3,4-di(octylphenyl)thiophene (**2e**) via a Suzuki coupling with dibromothiophene **2d**. Bis(methylene chloride) **2f** has been synthesized by a direct chloromethylation reaction. The last reaction step and purification toward monomer **2g** are identical to the first procedure.

Polymerization toward the Precursor Polymer. Both monomers were freeze-dried to remove any traces of water. The polymerizations have been initiated by different bases. All the other conditions are the same for every reaction; 2 equiv of base were used, the initial concentration of the monomer was fixed at 0.4 M and all polymerizations were performed at a definite reaction temperature (0 °C) and reaction time of 90 min.

To study the influence of the base on the formation of the precursor polymer, 4 different bases have been used: LHMDS, NaHMDS, KHMDS and Na*t*BuO.

The first base which has been tested is LHMDS. For this base, it has already been proven that the formation of high molecular weight materials is possible,[29] but the reproducibility of the polymerization showed to be an important problem. To test the reproducibility, over 20 experiments have been done. All the polymerizations were carried out under exactly the same conditions as described above. All the polymers reached a high molecular weight (Table 2), a moderated yield of 38% (average of all the experiments), but the achieved weight distribution differed significantly. Basically there are 3 different situations (Figure 1): a monomodal distribution (**1a**) (Figure 1), an intermediate situation which can be described as tailing (**1b**) and a bimodal distribution (**1c**). The monomodal distribution only occurred 2 times. Seemingly the polymerization process has the tendency to yield a bimodal distribution or tailing. Both situations appear in approximately the same frequency.

The different molecular weight distributions can be explained by the polymerization mechanism (Scheme 3). Polymerization starts with a base induced elimination from the (pre)monomer; the base abstracts a proton and subsequently one of the dithiocarbamate groups is expelled. This leads to the actual monomer, a *p*-quinodimethane system. The actual polymerization can proceed by either an anionic or radical mechanism (Scheme 3). In former work it has been shown

Scheme 1. Synthetic Route toward O-PTV[a]

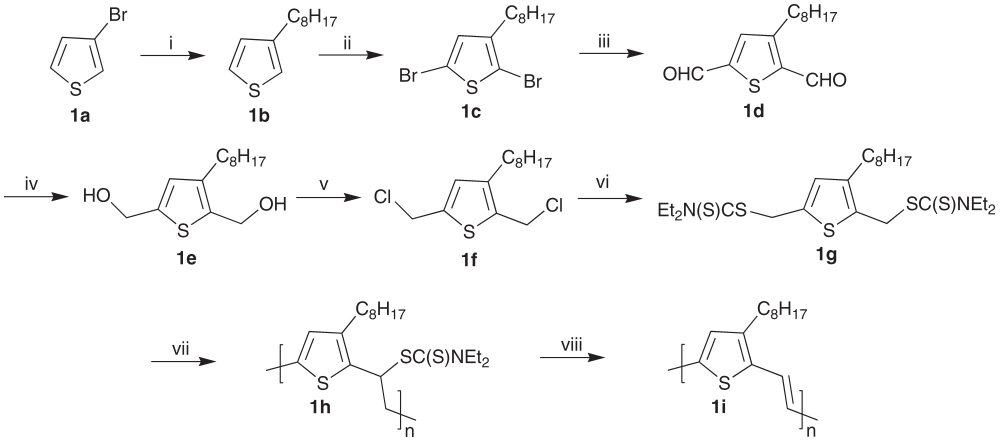

[a] Key: (i) $BrMgC_8H_{17}$, $NiCl_2$(dppp); (ii) NBS, DMF; (iii) (1) *n*-BuLi, (2) *n*-formylpiperidine; (iv) $LiAlH_4$, THF; (v) $SOCl_2$, THF; (vi) $NaSC(S)NEt_2 \cdot 3H_2O$, EtOH; (vii) base, THF; (viii) ΔT.

Scheme 2. Synthetic Pathway toward BOP-PTV[a]

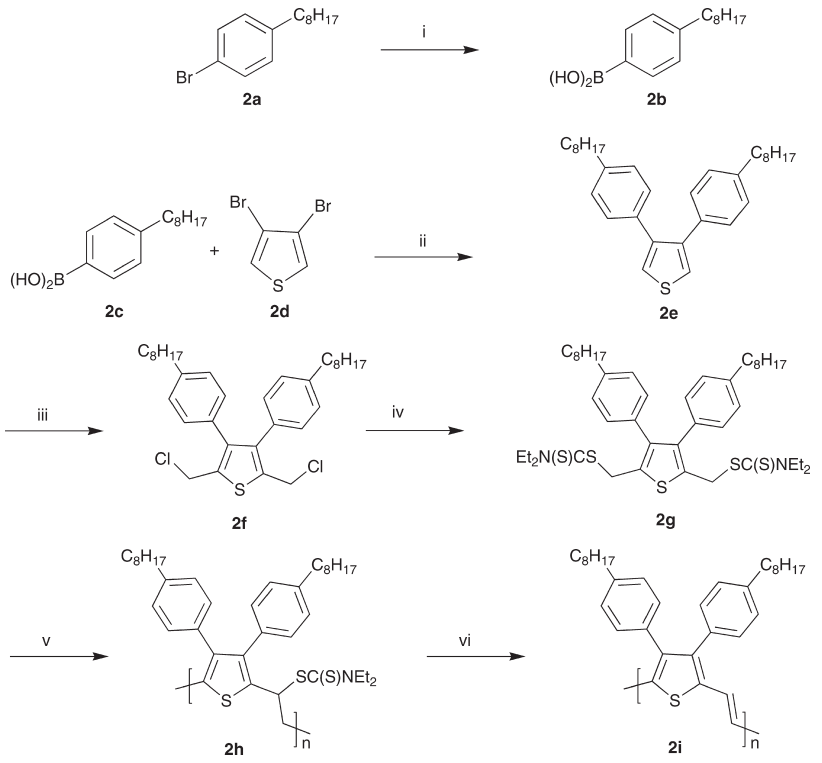

[a] Key: (i) 1. *n*-BuLi, 2. triisopropylborate; (ii) $Pd(PPh_3)_4$, KF, toluene/H_2O; (iii) CH_2O, HCl, Ac_2O; (iv) $NaSC(S)NEt_2 \cdot 3H_2O$, MeOH; (v) NaHMDS, THF; (vi) ΔT.

Table 2. Polymerization Results for the Precursor Polymer after Polymerization with LHMDS

entry	M_w (10^3)	PD	yield (%)
1	69	6.5	34
2	241	3.2	43
3	64	2.3	38
4	66	6.4	36
5	115	4.7	39
6	156	3	44
7	56	5.5	42
8	96	2.5	35
9	53	5.1	43
10	83	2	30

that the radical polymerization mechanism leads to the high molecular weight fraction and the anionic mechanism results in low molecular weight fractions.[36]

In case of the radical mechanism, the initiator is formed when two *p*-quinodimethane systems combine and a diradical originates. For the anionic mechanism a nucleophile has to be present as an initiator, it is possible that the base interacts as such a nucleophile or that the anionic intermediate toward the *p*-quinodimethane system takes up that role.[36]

To prove that two different polymerization mechanisms are present, two additional experiments have been done.[37] In a first experiment, 0.5 equiv of 2,2,6,6-tetramethylpiperidine-1-oxyl (TEMPO) has been added to a typical reaction mixture (Figure 2).[38] Here, the molecular weight has been reduced significantly (M_w, 28×10^3; PD, 6.4). This is an indication that the high molecular weights originate from a radical polymerization mechanism, which in this experiment is suppressed by the radical inhibitor, TEMPO. To verify this observation, a reversed addition, meaning that the monomer is added dropwise to a solution of the base, has been done (Figure 4). Such an addition should favor the anionic polymerization.[39,40] The experiment confirms this hypothesis, the molecular weight dropped extremely (M_w, 5.5×10^3; PD, 3.1).

The second base which has been used is the sodium equivalent of LHMDS, NaHMDS (Table 3 and Figure 3). Its base strength is conditioned by the basicity or the pK_a of the parent amine, hexamethyldisilazide. Even so, the results for these polymerizations differ significantly. Also high molecular weights have been reached. But now, all polymerizations have more or less the same bimodal distribution. Another advantage of the change of base is the fact that the yield rises until 52% (average of the four experiments).

To complete the sequence lithium−sodium−potassium, also the effect of KHMDS as a base has been tested. Here a monomodal distribution with lower molecular weights (M_w, 14×10^3, PD, 3.2) has been achieved, but the yield rises until 64% (Figure 4).

When we compare the three sterically hindered hexamethyldisilazane bases, the yield goes up through the sequence Li−Na−K. A second phenomenon that can be recognized concerns the molecular weight distribution. The larger the counterion (Li < Na < K), the more low molecular weight fractions are formed, so the anionic polymerization mechanism is in favor. A possible explanation can relate the results with differences in solvatation of the cation. The polymerizations are performed in THF, which is a solvent with a low dielectric constant (ε = 7.58)[41] and, therefore, a weakly dissociating solvent. In such a solvent the nucleophilicity of anions depends on the electrostatic attraction of the cation−anion pair and therefore the charge density on the cation. The larger the cation, the lower the charge density and the more the cation−anion pair will be separated. So the probability of any nucleophile to act as an anionic initiator increases.

Finally, sodium *tert*-butoxide has also been tested as a base. Its base strength is lower than LHMDS. This also leads

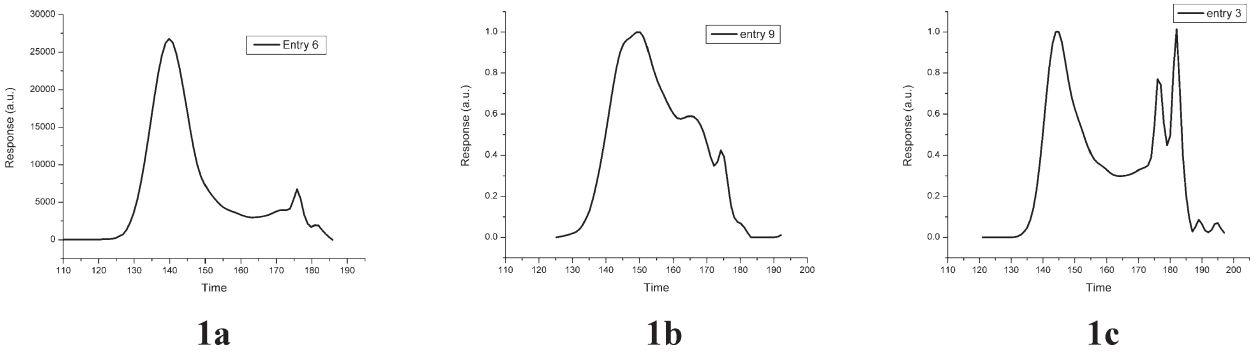

Figure 1. Molecular weight distribution of O-PTV (SEC profiles).

Scheme 3. Mechanism of Dithiocarbamate Monomer Polymerization via *p*-Quinodimethane System

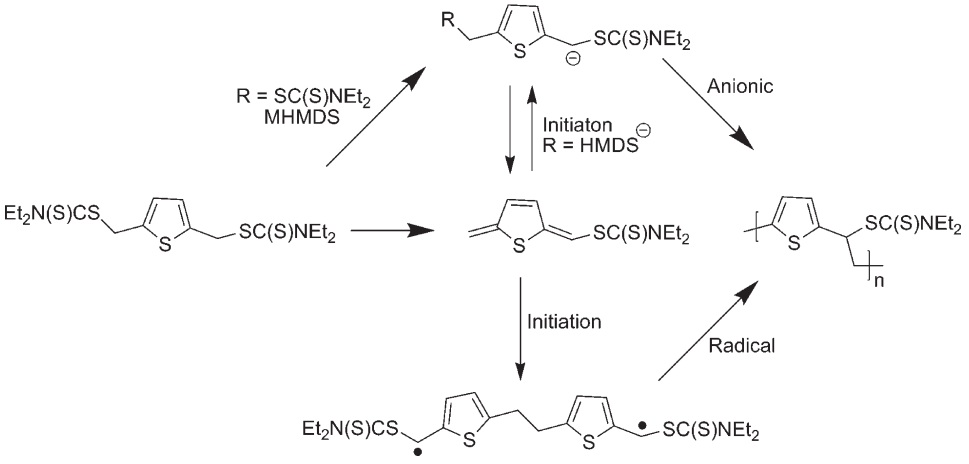

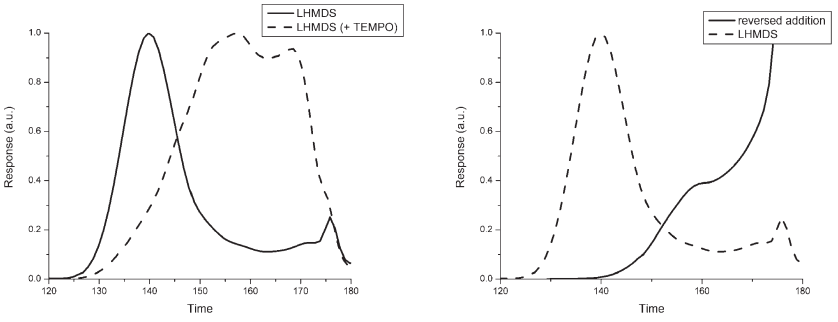

Figure 2. Influence of TEMPO and reversed addition on the molecular weight distribution.

to the formation of lower molecular weights ($M_w = 2 \times 10^3$) (Figure 5) under normal reaction conditions (0 °C). The high molecular weight peak is present in a very small amount. From previous experience[42] it is indeed to be expected that due to the lower base strength, proton abstraction and formation of the *p*-quinodimethane system is much slower. In case of a competition between a radical and an anionic mechanism the competition occurs at the level of initiation kinetics.[39] As the rate of initiation for the radical mechanism scale with the square and for the anionic mechanism in first order in the concentration of the *p*-quinodimethane system, initiation kinetics are for the former more sensitive to concentration of the true monomer than the latter.

Consequently, this would imply that higher temperatures leading to a more efficient formation of the true monomer and keeping all other polymerization parameters (time, equivalents base, ...) constant, would lead to a more competitive radical polymerization mechanism. Accordingly performing the polymerization reaction at 35 and 60 °C results in an increased contribution of the high molecular weight fraction (Figure 5). The molecular weights observed at 202×10^3 and 164×10^3 Da, respectively, stay virtually constant.

Table 3. Polymerization Results with NaHMDS

	high molecular weight		low molecular weight		
entry	M_w (10^3)	PD	M_w (10^3)	PD	yield
1	164	2	2.0	1.2	50
2	107	1.9	2.4	1.3	51
3	218	2.8	2.7	1.5	54
4	208	2.6	2.7	1.4	52

The precursor polymers which are used for further characterization have been made in the same conditions. Both monomers (**1g** and **2f**) were polymerized using sodium

hexamethyldisilazide (2 M solution in THF) as a base in dry THF at 0 °C for 90 min to afford the polymers (**1g** and **2f**).

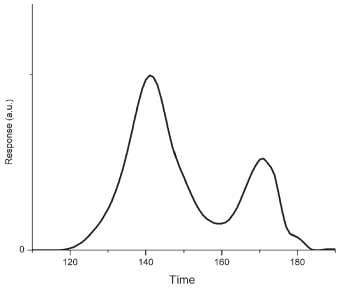

Figure 3. SEC profile (entry 4) for polymerization with NaHMDS.

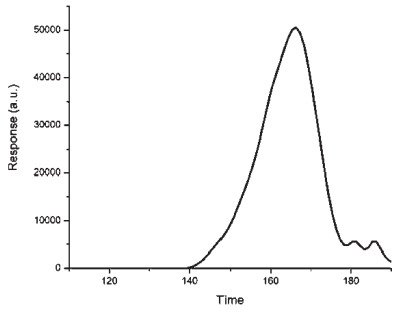

Figure 4. SEC profile for polymerization with KHMDS.

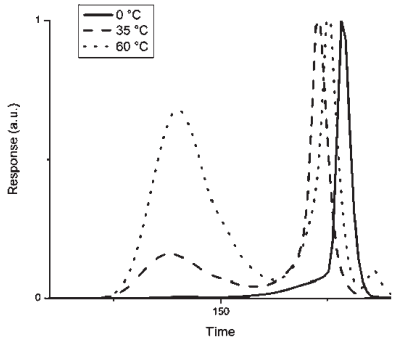

Figure 5. SEC profiles for polymerization at 0, 35, and 60 °C.

Table 4. SEC Data for the Precursor and the Conjugated Polymers

	M_w	PD
O-PTV precursor polymer	86×10^3	3.1
O-PTV	65×10^3	2.6
BOP precursor polymer	186×10^3	2.7
BOP PTV	53×10^2	2.1

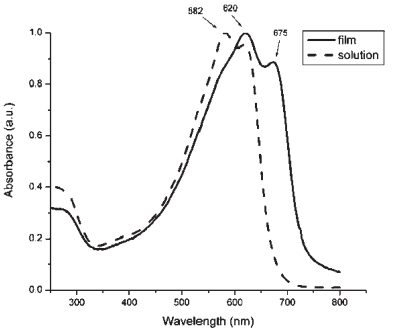

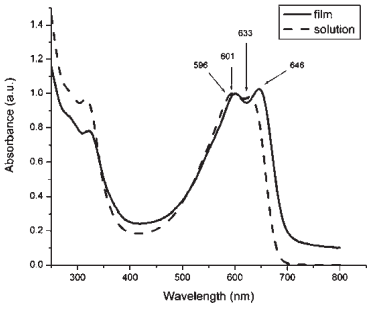

Figure 6. UV−vis spectra of the conjugated polymers (film and solution).

Workup and purification have been done as described above. The isolated yields range from 56% for the octyl-precursor polymer to 54% for the BOP-precursor polymer. Molecular weights were determined by means of SEC in THF against polystyrene standards (Table 4).

Conversion to the Conjugated Polymers. The precursor polymers can be converted into their conjugated counterparts by a thermal treatment (Scheme 1 and 2). Upon heating, the dithiocarbamate group of the precursor polymer is eliminated to form the conjugated backbone. The thermal conversion has been performed in solution. The precursor polymers are dissolved in *o*-dichlorobenzene and stirred for 4.5 h at 180 °C to form O-PTV and at 150 °C to form BOP-PTV. Polymers are isolated by precipitation of the resulting reaction mixture in MeOH. After isolation the conjugated polymers were characterized by UV/vis (Figure 6) and SEC (Table 4). Furthermore, the polymers were studied by FT-IR spectroscopy, to be certain that all dithiocarbamate groups disappeared and therefore full conjugation has been realized.

Transport Properties. Hole only devices have been made resulting in a hole mobility of 3×10^{-9} $m^2/(V\,s)$ for BOP-PTV and 5×10^{-9} $m^2/(V\,s)$ for O-PTV, which is slightly lower as compared to the hole mobility of 3×10^{-8} $m^2/(V\,s)$ for P3HT, but nevertheless acceptable when compared to other efficient low band gap donors (Figure 7).[8,43−45] Combined with the good transport properties of PCBM no space charge effects are expected, at least for moderately thick films, similar to those used in MDMO-PPV:PCBM blends.

Cyclic Voltammetry. The cyclic voltammograms of thin films of BOP-PTV and O-PTV display distinct characteristic irreversible oxidation and reduction processes during the

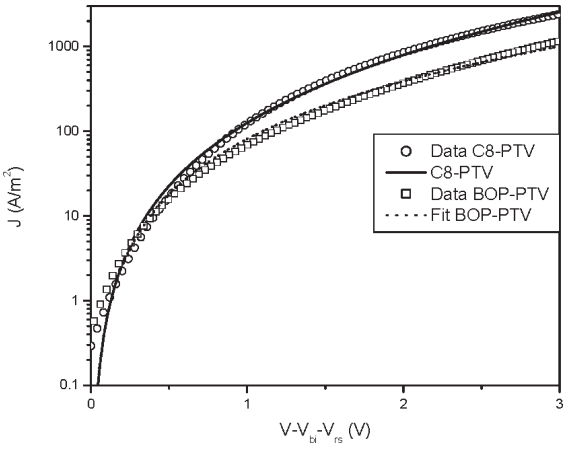

Figure 7. Current density versus voltage, corrected for built in voltage and series resistance of a BOP-PTV and O-PTV hole only device. Data (symbols) are fitted (line) using a space charge limited current with a field dependent mobility.

first potential scan. Upon repeated scanning the currents associated with these features significantly reduces, as expected for irreversible electrochemical processes. From the onset potentials of the oxidation and reduction the position of the energy levels can be estimated. For BOP-PTV the onset of oxidation occurs at 0.46 V vs $Ag/AgNO_3$ and the onset of reduction occurs at −1.18 V vs $Ag/AgNO_3$. The corresponding energy level of BOP-PTV for the highest occupied molecular orbital (HOMO) is −5.39 eV and for the lowest unoccupied molecular orbital (LUMO) is −3.75 eV. For O-PTV the onset of oxidation occurs at 0.22 V vs $Ag/AgNO_3$ and the onset of reduction occurs at −1.30 V vs $Ag/AgNO_3$. The corresponding energy level of O-PTV for the highest occupied molecular orbital (HOMO) is −5.15 eV and for the lowest unoccupied molecular orbital (LUMO) is −3.63 eV. The resulting electrochemical band gap of BOP-PTV is 1.64 eV and of O-PTV is 1.52 eV. Although in the same order of magnitude, these values are somewhat lower than the observed optical band gaps (1.78 and 1.70 eV, respectively). This is not surprising, since the determination of the onsets of oxidation and reduction for irreversible electrochemical processes may incur some level of error. Notwithstanding, the cyclic voltammetry measurements clearly confirm the occurrence of a lower band gap for O-PTV as compared to BOP-PTV, likely a result of increased conformational disorder due to steric effects of the substituents. In addition, for BOP-PTV both the HOMO and the LUMO are lowered as compared to O-PTV, which reflects the electronic effects of the phenyl substituents (Table 5).

Solar Cells. Solar cells were made by sandwiching the conjugated polymers in between an ITO/PEDOT:PSS anode and a samarium/aluminum cathode. The best obtained performance for bulk heterojunction solar cells with BOP-PTV or O-PTV as donor polymer and PCBM as acceptor material are depicted in Figure 8 and Table 6. For a 1:4 BOP-PTV:PCBM solar cell spin coated from chloroform the highest achieved efficiency is 0.80%. This cell has an open circuit voltage (V_{oc}) of 0.67 V and a fill factor of 60% and higher for films with a thickness of more than 200 nm, indicating good charge transport properties of the blend. For a 1:4 O-PTV:PCBM solar cell spin coated from *o*-dichlorobenzene the highest achieved efficiency is 0.92%. The open circuit voltage (V_{oc}) of O-PTV is 0.47 V, this is 0.2 V less compared to BOP-PTV.

Table 5. CV Data for O-PTV and BOP-PTV

	HOMO	LUMO	E_g (electrochemical)	E_g (optical)
O-PTV	−5.15	−3.63	1.52	1.70
BOP-PTV	−5.39	−3.75	1.64	1.78

This difference in V_{oc} is most likely originated from the differences in the HOMO levels of both polymers. Apparently, the introduction of phenyl substituents results in a lowering of the HOMO energy level, which translates itself in a larger V_{oc}. The difference in short circuit currents can be explained by the differences in absorption of both films, which will be discussed in the next section. Notwithstanding, the short circuit currents (J_{sc}) are low, which results in the observed efficiencies below 1.0%. Even so the performance of the solar cells made by the optimized polymerization with NaHMDS are significant better than the one made by LHMDS. Girotto et all measured an efficiency of 0.15% −0.17% for other 3-alkyl-substituted PTV's.[46] So by optimizing the synthetic route toward the PTV-derivatives, the efficiency of the solar cell has been increased by a factor of 4.5.

Absorption Characteristics. To understand the moderate efficiencies for these new low band gap polymers, the absorption characteristics, in solution as well as in thin films, of both PTV derivatives have been studied and compared to P3HT. To this end, thin films of P3HT, BOP-PTV, and O-PTV were prepared from the same solvent, i.e., chloroform. After measuring the film thickness, the absolute absorbance as a function of the wavelength can be readily determined (Figure 9). Furthermore, the optical band gap can be derived from the low energy side tangent to the $\pi-\pi^*$ transition. The band gap and the absolute absorptivity in a thin film are presented in Table 7.

The moderate short circuit currents (J_{sc}) of BOP-PTV and O-PTV compared to P3HT can be understood in terms of the absolute absorption maxima. It is noteworthy that the absorptivity of P3HT and O-PTV in a thin film follow the same trend relative to the molar attenuation coefficient. On the other hand where BOP-PTV has the highest molar attenuation coefficient of the three compounds, this does not translate to a high absorptivity. This can be explained in part by the high structural order and even crystalline character of P3HT[47] and the expected nature or rotational disorder of the larger side chains in BOP-PTV. This will be a subject for further research.

Table 6. Solar Cell Performance for BOP-PTV:PCBM and O-PTV:PCBM

	V_{oc} (V)	J_{sc} (A/m^2)	FF %	Efficiency %
1:4 O-PTV:PCBM	0.47	52.8	35	0.92
1:1 BOP-PTV:PCBM	0.66	9.1	59	0.34
1:2 BOP-PTV:PCBM	0.67	15.8	57	0.66
1:4 BOP-PTV:PCBM	0.67	18.3	60	0.80

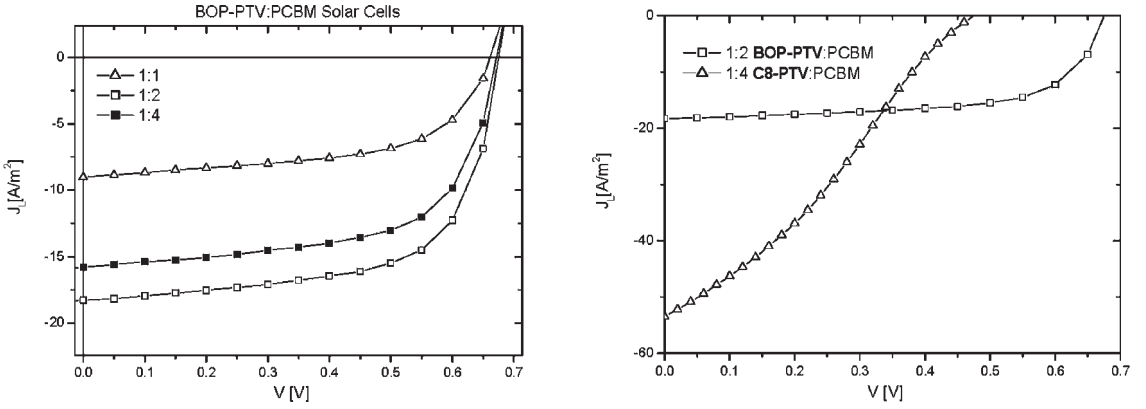

Figure 8. Current density versus voltage of PTV:PCBM solar cells under illumination of a 1000 W/m^2 simulated solar spectrum.

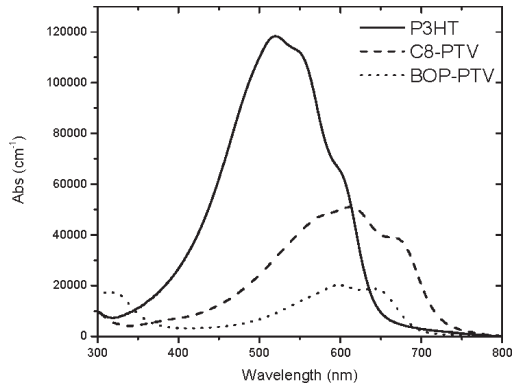

Figure 9. Absolute absorbance in function of the wavelength for spin-coated films of P3HT, BOP-PTV, and O-PTV.

Table 7. Thin Film Absolute Absorptivities, Solution Extinction Coefficients, and Optical Band Gaps of BOP-PTV, O-PTV, and P3HT

	thin film absolute absorptivity (cm^{-1})	molar attenuation coefficient (M^{-1} cm^{-1})	optical band gap (eV)
BOP-PTV	20 135	10 453	1.78
O-PTV	50 998	4240	1.70
P3HT	118 334	8000	1.90

Conclusions

In conclusion, two new conjugated polymers were synthesized via the dithiocarbamate precursor route. Synthesis of the required substituted thiophene dithiocarbamate monomers was easily achieved. The polymerization has been optimized by the use of 4 different bases. Polymerizations with NaHMDS as a base resulted in polymers with high molecular weights, high λ_{max} values, acceptable polydispersities and more important a good reproducibility. Both polymers were provided with alkyl side chains to guarantee solubility and improve the processing capacities: therefore we have a better solar cell performance than for the unsubstituted PTV. It is demonstrated that these narrow band gap polymers have a sufficiently high hole mobility. Notwithstanding, the short circuit currents (J_{sc}) are still inferior, resulting in low efficiencies. The moderate short circuit currents (J_{sc}) of BOP-PTV and O-PTV compared to P3HT can be explained by their significant lower absorptivity in thin films.

Acknowledgment. The authors gratefully acknowledge BELSPO in the frame of network IAP P6/17, and the Fund for Scientific Research, Flanders (Belgium) (FWO) for financial support and for granting Ph.D. fellowships (H.D. and A.P.). The FWO is also gratefully acknowledged for the funding of the project G.0091.07. We also thank the European Science Foundation (ESF) for the received support for the activity entitled "New Generation of Organic based Photovoltaic Devices".

References and Notes

(1) Mayer, A. C.; Scully, S. R.; Hardin, B. E.; Rowell, M. W.; McGehee, M. D. *Mater. Today* **2007**, *10*, 28–33.
(2) Winder, C.; Sariciftci, N. S. *J. Mater. Chem.* **2004**, *14*, 1077–1086.
(3) Goris, L.; Loi, M. A.; Cravino, A.; Neugebauer, H.; Sariciftci, N. S.; Polec, I.; Lutsen, L.; Manca, J.; De Schepper, L.; Vanderzande, D. *Synth. Met.* **2003**, *138*, 249–253.
(4) Colladet, K.; Nicolas, M.; Goris, L.; Lutsen, L.; Vanderzande, D. *Thin Solid Films* **2004**, *7*, 451–452.
(5) Shaheen, S. E.; Vangeneugden, D.; Kiebooms, R.; Vanderzande, D.; Fromherz, T.; Padinger, F.; Brabec, D. J.; Sariciftci, N. S. *Synth. Met.* **2001**, *121*, 1583–1584.
(6) Koster, L. J. A.; Mihailetchi, V. D.; Blom, P. W. M. *Appl. Phys. Lett.* **2006**, *88*, 93511−1–93511−3.
(7) Scharber, M. C.; Mühlbacher, D.; Koppe, M.; Denk, P.; Waldauf, C.; Heeger, A. J.; Brabec, C. J. *Adv. Mater.* **2006**, *18*, 789–794.
(8) Henckens, A.; Colladet, K.; Fourier, S.; Cleij, T. J.; Lutsen, L.; Gelan, J.; Vanderzande, D. *Macromolecules* **2005**, *38*, 19–26.
(9) Yeon-Beom, L.; Hong-Ku, S.; Seung-Won, K. *Macromol. Rapid Commun.* **2003**, *24*, 522–526.
(10) Kroon, R.; Lenes, M.; Hummelen, J. C.; Blom, P. W. M.; De Boer, B. *Polym. Rev.* **2008**, *48*, 531–582.
(11) Van De Wetering, K.; Brochon, C.; Nhov, C.; Hadziioannou, G. *Macromolecules* **2006**, *39*, 4289–4297.
(12) Vanderzande, D. J.; Issaris, A. C.; Van Der Borght, M. J.; van Breemen, A. J.; de Kok, M. M.; Gelan, J. M. *Macromol. Symp.* **1998**, *125*, 189–203.
(13) Feast, W. J.; Winter, J. N. *J. Chem. Soc., Chem. Commun.* **1985**, *4*, 202–203.
(14) Helgesen, M.; Gevorgyan, S. A.; Krebs, F. C.; Janssen, R. A. J. *Chem. Mater.* **2009**, *21*, 4669–4675.
(15) Helgesen, M.; Krebs, F. C. *Macromolecules* **2010**, *43*, 1253–1260.
(16) Harper, K.; West, W. J. W. Eur. Pat. Appl. No. 182548, 1985.
(17) Jen, K. Y.; Jow, R.; Eckhardt, H.; Elsenbaumer, R. L. *Polym. Mater. Sci. Eng.* **1987**, *56*, 49–53.
(18) Jen, K. Y.; Maxfield, M.; Shacklette, L. W.; Elsenbaumer, R. L. *J. Chem. Soc., Chem. Commun.* **1987**, 309–311.
(19) Yamada, D.; Tokito, S.; Tsutsui, T.; Saito, S. *J. Chem. Soc., Chem. Commun.* **1987**, *00*, 1448–1449.
(20) Tokito, S.; Momii, T.; Murata, H.; Tsutsui, T.; Saito, S. *Polymer* **1990**, *31*, 1137–1141.
(21) Tsutsui, T.; Murata, H.; Momii, T.; Yoshiura, K.; Tokito, S.; Saito, S. *Synth. Met.* **1991**, *41*, 327–330.
(22) Murase, I.; Ohnishi, T.; Noguchi, T. *Ger. Offen.* No. 3704411, **1987**.
(23) Henckens, A.; Knipper, M.; Polec, I.; Manca, J.; Lutsen, L.; Vanderzande, D. *Thin solid films* **2004**, *451−452*, 472–579.
(24) Henckens, A. Ph.D. dissertation, University of Hasselt: Diepenbeek, Belgium, October 2003.
(25) Mitchell, W. J.; Pena, C.; Burn, P. L. *J. Mater. Chem.* **2002**, *12*, 200–205.
(26) Henckens, A.; Lutsen, L.; Vanderzande, D.; Knipper, M.; Manca, J. *J. SPIE Proc.* **2004**, 52–59.
(27) Banishoeib, F.; Fourier, S.; Cleij, T. J.; Lutsen, L.; Vanderzande, D. *Eur. Phys. J.: Appl. Phys.* **2007**, *37*, 237–240.
(28) Nguyen, L. H.; Günes, S.; Neugebauer, H.; Sariciftci, N. S.; Banishoeib, F.; Henckens, A.; Cleij, T. J.; Lutsen, L.; Vanderzande, D. *Sol. Energ. Mat. Sol. C.* **2006**, *90*, 2815–2828.
(29) Banishoeib, F.; Adriaensens, P.; Berson, S.; Guillerez, S.; Douheret, O.; Manca, J.; Fourier, S.; Cleij, T. J.; Lutsen, L.; Vanderzande, D. *Sol. Energ. Mat. Sol. C.* **2007**, *91*, 1026–1034.
(30) Banishoeib, F.; Henckens, A.; Fourier, S..; Vanhooyland, G.; Breselge, M.; Manca, J.; Cleij, T. J.; Lutsen, L.; Vanderzande, D.; Nguyen, L. H.; Neugebauer, H.; Sariciftci, N. S. *Thin solid films* **2008**, *516*, 3978–3988.
(31) Tamao, K.; Kodama, S.; Nakajima, I.; Kumada, M. *Tetrahedron* **1982**, *38*, 3347–3354.
(32) Bäuerle, P.; Pfau, F.; Schlupp, H.; Würthner, F.; Gaudl, K. U.; Caro, M. B.; Fischer, P. *J. Chem. Soc. Perk. T. 2* **1993**, 489–494.
(33) Frey, J.; Bond, A. D.; Holmes, A. B. *Chem. Commun.* **2002**, 2424–2425.
(34) Becker, H.; Spreitzer, H.; Ibrom, K.; Kreuder, W. *Macromolecules* **1999**, *32*, 4925–4932.
(35) Wand, M. D.; Thurmes, W. N.; Walba, D. M. US patent 5,380,460, 1995.
(36) Henckens, A.; Duyssens, I.; Lutsen, L.; Vanderzande, D.; Cleij, T. J. *Polymer* **2006**, *47*, 123–131.
(37) Vandenbergh, J.; Wouters, J.; Adriaensens, P. J.; Mens, R.; Cleij, T. J.; Lutsen, L.; Vanderzande, D. *Macromolecules* **2009**, *42*, 3661–3668.
(38) Hontis, L.; Van Der Borght, M.; Vanderzande, D.; Gelan, J. *Polymer* **1999**, *40*, 6615–6617.
(39) Vanderzande, D. J. M.; Hontis, L.; Palmaerts, A.; Van Den Berghe, D.; Wouters, J.; Lutsen, L.; Cleij, T. *Proc. SPIE* **2005**, *5937*, 59370Q-1–59370Q-10.
(40) Neef, C. J.; Ferraris, J. P. *Macromolecules* **2000**, *33*, 2311–2314.
(41) Riddick, J. A.; Bunger, W. B.; Sakano, T. K. *Org. Sol.: Phys. Prop. Methods Purif.* **1986**, 309–311.
(42) Adriaensens, P.; Van Der Borght, M.; Hontis, L.; Issaris, A.; van Breemen, A.; de Kok, M.; Vanderzande, D.; Gelan, J. *Polymer* **2000**, *41*, 7003–7009.

(43) Andersson, L. M.; Zhang, F. L.; Inganas, O. *Appl. Phys. Lett.* **2006**, *89*, 142111.
(44) Zhang, F. L.; Mammo, W.; Andersson, L. M. *Adv. Mater.* **2006**, *18*, 2169–2173.
(45) Mihailetchi, V. D.; Xie, H.; De Boer, B.; Koster, L. J. A.; Blom, P. W. M. *Adv.Funct. Mater.* **2006**, *16*, 699–708.
(46) Girotto, C.; Cheyns, D.; Aernouts, T.; Banishoeib, F.; Lutsen, L.; Cleij, T. J.; Vanderzande, D.; Genoe, J.; Poortmans, J.; Heremans, P. *Org. Electron.* **2008**, *9*, 740–746.
(47) Oosterbaan, W. D.; Vrindts, V.; Berson, S.; Guillerez, S.; Douhéret, O.; Ruttens, B.; D'Haen, J.; Adriaensens, P.; Manca, J.; Lutsen, L.; Vanderzande, D. *J. Mater.Chem.* **2009**, *19*, 5424–5435.